Preparation and Characterization of (Tetrabenzoporphyrinato)nickel Hexafluoroarsenate, $(NiTBP)_3(AsF_6)_2(C_{10}H_7Cl)$. A New Type of Metallomacrocyclic Radical Salts

Kyuya YAKUSHI,* Michiko YOSHITAKE, Haruo KURODA, Atsushi KAWAMOTO,†
Jiro TANAKA,† Tadashi SUGANO,†† and Minoru KINOSHITA††
Department of Chemistry, Faculty of Science, the University of Tokyo, Hongo, Tokyo 113
†Department of Chemistry, Faculty of Science, Nagoya University, Furocho, Chikusa-ku, Nagoya 474
††Institute for Solid State Physics, the University of Tokyo, Roppongi, Tokyo 106
(Received November 5, 1987)

Single crystals of a (tetrabenzoporphyrinato)nickel hexafluoroarsenate, $(NiTBP)_3(AsF_6)_2$ were prepared by the use of an electrochemical technique. NiTBP is stacked one-dimensionally with a periodic unit composed of three macrocycles. This stacking mode is a new type among the one-dimensionally stacked macrocyclic complexes. The experimental results on reflectance spectrum and ESR indicate that this material is a one-dimensional semiconductor with a small electron correlation.

Study on highly conducting quasi-one-dimensional solids of metallomacrocyclic compounds has been extensively conducted by the group of Northwestern University.[1-7] They explored mainly iodine complexes by changing the central metals from Fe to Zn. They also studied on (tetrabenzoporphyrinato)nickel iodide. The family of the one-dimensionally stacked macrocycles will be expanded by selecting the combination of the central metals, the porphyrin ligands, and the counter anions. We have prepared metallic (phthalocyaninato)nickel salts by the use of an electrochemical technique to change the counter anions, and found a new complexes with a different chemical composition from iodine complexes.[8,9] This time we prepared a one-dimensional complex by using a (tetrabenzoporphyrinato)nickel as a macrocycle and several octahedral, tetrahedral, and linear anions as counter anions. In this paper we present the crystal structure, electrical, optical, and magnetic properties of $(NiTBP)_3(AsF_6)_2(C_{10}H_7Cl)$, and briefly describe the preliminary results on the other salts.

Experimental

NiTBP was synthesized by exchanging the central metal of ZnTBP according to the method given by Martinsen et al.,[6] and was purified by means of vacuum sublimation. The result of the chemical analysis was as follows; Found: C, 76.07; H, 3.42; N, 9.79, Calcd for $C_{36}H_{20}N_4Ni$: C, 76.22; H, 3.55; N, 9.88. Single crystals of the NiTBP radical salts were grown by oxidizing NiTBP electrochemically in the 1-chloronaphthalene solution, $(n\text{-}Bu)_4X$ (X=BF_4, ClO_4, ReO_4, PF_6, AsF_6, SbF_6, Br_3, I_3) being used as the supporting electrolytes. 1-Chloronaphthalene were refluxed with CaH_2 under the Ar atmosphere and then distilled in vacuum. The electrolytes were recrystallized from methanol solution for several times. The electrochemical oxidation were performed at 120±2 °C with a constant current of 2—5 μA for about two weeks. The concentrations of NiTBP and the electrolytes were 2×10^{-4} mol l^{-1} and 1.6×10^{-3} mol l^{-1}, respectively. NiTBP is more soluble to 1-chloronaphthalene than NiPc ((phthalocyaninato)nickel), and almost all NiTBP seems to be consumed after two weeks because the deep color of the starting material disappeared. The needle-

Table 1. Crystal Data

Compound	$(NiTBP)_3(AsF_6)_2(C_{10}H_7Cl)$
Formula	$(NiC_{36}H_{20}N_4)_3(AsF_6)_2(C_{10}H_7Cl)$
Formula wt.	2242.23
Cell parameters a	16.019(2) Å
b	16.470(3) Å
c	9.853(5) Å
α	108.30(2)°
β	96.10(3)°
γ	66.06(1)°
Cell volume V	2255.0 Å^3
Number of formula unit Z	1
Density: calcd.	1.65 g cm^{-3}
Density: obsd.	1.57 g cm^{-3}
Space group	$P\bar{1}$
Radiation	Cu $K\alpha$
Linear absorption coefficient	25.5 cm^{-1}
Crystal shape	needle-like elongated along c-axis
Number of reflections ($F_o > 3(\sigma(F_o))$)	6202
R-factor	0.083

Table 2. Fractional Coordinates ($\times 10^4$) and Equivalent Temperature Factors ($B_{eq}=(4/3)\sum_{ij}\beta_{ij}a_ja_i$)

	x	y	z	B_{eq}
NiTBP molecule A				
Ni(1)	0	0	0	1.8
N(2)	−641(3)	−854(3)	−594(5)	1.8
N(3)	1173(3)	−1073(4)	−95(5)	1.8
C(4)	−1565(4)	−621(4)	−805(6)	2.1
C(5)	−1772(5)	−1451(5)	−1253(7)	2.4
C(6)	−2604(5)	−1553(6)	−1589(9)	3.6
C(7)	−2545(6)	−2478(6)	−1996(10)	4.3
C(8)	−1712(6)	−3230(6)	−2053(10)	4.0
C(9)	−881(5)	−3113(5)	−1716(8)	3.1
C(10)	−952(5)	−2197(5)	−1314(7)	2.4
C(11)	−256(4)	−1801(4)	−898(6)	2.0
C(12)	655(4)	−2360(5)	−845(7)	2.3
C(13)	1321(4)	−2000(4)	−469(6)	2.0
C(14)	2276(4)	−2581(5)	−403(7)	2.4
C(15)	2739(5)	−3541(5)	−707(8)	3.2
C(16)	3694(5)	−3878(6)	−549(9)	4.0
C(17)	4149(5)	−3269(6)	−115(9)	3.8
C(18)	3682(5)	−2304(5)	176(8)	3.2
C(19)	2727(4)	−1978(5)	20(7)	2.4
C(20)	2037(4)	−1050(5)	204(6)	2.1
C(21)	2224(4)	−263(5)	625(7)	2.2
NiTBP molecule B				
Ni(22)	−317(1)	196(1)	3282(1)	2.0
N(23)	−1604(3)	345(4)	2924(5)	2.0
N(24)	65(3)	−1160(4)	2790(5)	1.9
N(25)	963(4)	41(4)	3648(5)	2.0
N(26)	−711(4)	1563(4)	3774(5)	2.1
C(27)	−2354(4)	1166(5)	3020(7)	2.6
C(28)	−3180(5)	976(5)	2636(7)	2.8
C(29)	−4087(5)	1570(7)	2535(10)	4.5
C(30)	−4710(6)	1136(7)	2088(12)	5.5
C(31)	−4437(6)	171(7)	1780(11)	4.8
C(32)	−3539(5)	−408(6)	1877(9)	4.0
C(33)	−2909(5)	24(5)	2311(7)	2.7
C(34)	−1926(5)	−361(5)	2482(7)	2.5
C(35)	−1419(5)	−1292(5)	2245(7)	2.5
C(36)	−485(5)	−1660(5)	2378(7)	2.3
C(37)	58(5)	−2653(5)	2101(7)	2.6
C(38)	−180(6)	−3426(6)	1663(9)	3.7
C(39)	535(6)	−4285(6)	1445(10)	4.2
C(40)	1446(6)	−4398(6)	1667(9)	4.1
C(41)	1673(5)	−3613(5)	2142(8)	3.3
C(42)	953(5)	−2750(5)	2348(7)	2.5
C(43)	943(4)	−1815(5)	2770(7)	2.2
C(44)	1727(5)	−1649(5)	3108(7)	2.4
C(45)	1720(4)	−762(5)	3503(6)	2.3
C(46)	2551(5)	−587(5)	3822(7)	2.6
C(47)	3466(5)	−1181(6)	3752(8)	3.5
C(48)	4112(6)	−779(7)	4047(10)	4.5
C(49)	3822(6)	194(7)	4418(10)	4.5
C(50)	2904(5)	799(6)	4516(8)	3.6
C(51)	2274(5)	371(5)	4180(7)	2.6
C(52)	1291(5)	760(5)	4067(6)	2.3
C(53)	773(5)	1686(5)	4330(7)	2.4
C(54)	−148(5)	2050(5)	4167(7)	2.5
C(55)	−687(5)	3036(5)	4405(7)	2.8
C(56)	−426(6)	3807(5)	4753(9)	4.0
C(57)	−1115(7)	4665(6)	4802(11)	5.0
C(58)	−2038(7)	4783(6)	4540(10)	4.6
C(59)	−2289(6)	4024(5)	4221(9)	3.8
C(60)	−1590(5)	3150(5)	4156(7)	2.7
C(61)	−1586(5)	2216(5)	3764(7)	2.5
C(62)	−2364(5)	2042(5)	3429(7)	2.6
AsF_6 anion				
As(63)	3119(1)	3286(1)	8073(2)	7.1
F(64)	3080(13)	3134(9)	6350(13)	20.5
F(65)	3042(13)	3511(9)	9781(13)	22.2
F(66)	2147(9)	4222(8)	8167(16)	17.0
F(67)	4013(9)	2383(8)	7937(22)	22.9
F(68)	3593(13)	3982(11)	8259(24)	26.3
F(69)	2561(9)	2639(10)	7970(22)	22.1
1-Chloronaphthalene				
Cl(70)	−5986(8)	3985(9)	3008(16)	10.5
C(71)	−5000	5000	5000	9.4
C(72)	−4541(14)	3864(12)	6828(21)	5.4
C(73)	−4363(11)	4489(13)	7077(20)	12.6
C(74)	−5305(19)	3758(17)	5226(35)	10.6
C(75)	−4095(15)	5192(20)	7319(30)	10.1
C(76)	−5454(17)	4144(20)	4380(28)	11.1
C(77)	−4900(18)	4302(22)	5787(35)	11.2
C(78)	−4438(19)	5234(22)	6303(32)	11.5

like crystal was elongated to the c-axis developing {100}, {010}, and {110} planes. The chemical analysis of Ni and As in the crystal were conducted by the use of the ICP atomic emission spectrometer, Jarrel Ash ICAP-575II.

The intensities of X-ray diffraction were collected with a Rigaku automated diffractometer using Cu $K\alpha$ radiation monochromatized with a graphite plate. The crystal data were listed in Table 1. The structure was solved by the heavy atom method and was refined by the block-diagonal least-squares method. All hydrogen atoms were neglected in the analysis. The absorption collection was made with a program ACACA written by C. T. Prewitt. R-value was 11.7% without a solvent molecule. The difference synthesis map revealed that solvent molecules are included in the crystal and the solvent molecule was located around (1/2, 1/2, 1/2) in the unit cell. Since the solvent molecule was disordered around the center of symmetry, two atoms, Cl(70) and C(71), overlap other carbon atoms related by the inversion symmetry. In order to avoid the divergence of the overlapped atoms, we refined Cl(70) by using an average atomic scattering factor between chlorine and carbon, and fixed the positional parameters of C(71) at the inversion center. Therefore, the geometry of 1-chloronaphthalene was determined to be heavily distorted. The final R-value decreased to 8.3% by refining the parameters of 1-chloronaphthalene. The molecular geometry of NiTBP did not change significantly before and after including a solvent molecule in the analysis. The temperature factor of fluorine atoms of AsF_6 is very large probably due to the orientational disorder, so that the positions of fluorine atoms could not be accurately determined. Since we are mainly interested in the column structure of NiTBP, we stopped the analysis at this

stage. The final atomic coordinates were shown in Table 2. The computer program used in this analysis was the UNICS system.[10]

The electrical resistivity was measured along the needle axis by using a two-probe method. The contact between the sample and the 20 μm gold wire were made by carbon paint. The polarized reflectance spectrum of the single crystal were measured in the spectral region from 2000 cm^{-1} to 25000 cm^{-1} by using a microspectro-photometric technique.[11,12] ESR were measured with JEOL, JES-FElXG by the use of X-band.

Results and Discussion

$(NiTBP)_3(AsF_6)_2(C_{10}H_7Cl)$. The ratio of the chemical composition between NiTBP and AsF_6 was determined to be 1.4±0.1:1 by means of ICP atomic emission spectrometry of Ni and As atoms. The 3:2 composition was supported also by crystal structure analysis. This chemical composition between a macrocycle and a counter anion is a new one in the family of the radical salts based on the metallo-macrocyclic compounds. Figure 1 shows the side view of the molecular columns of NiTBP. NiTBP's are stacking along the c-axis with their molecular planes parallel to each other. The unit of this molecular column is a trimer of NiTBP which is composed of a molecule, A, on the center of symmetry and two molecules, B and B′, which are interrelated by the center of symmetry. The dihedral angle between the molecules A and B is 0.6°. Table 3 shows the mean bond lengths which were calculated by averaging the chemically equivalent bonds. Significant difference in the molecular geometry was not observed between the molecules A and B, and also between the molecules of $(NiTBP)_3(AsF_6)_2(C_{10}H_7Cl)$ and NiTBPI.[6] The neighboring molecules within the trimer is overlapping with a twisted angle of 45.0° as shown in

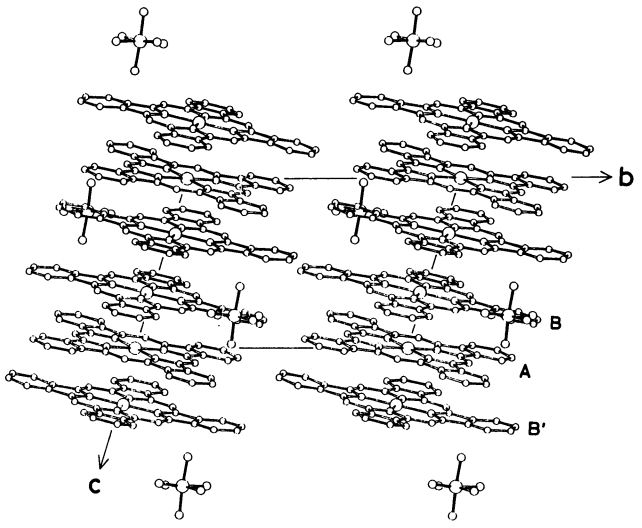

Fig. 1. Side view of the molecular columns of NiTBP. The solvent molecule included in the crystal at (1/2, 1/2, 1/2) is not drawn in this figure.

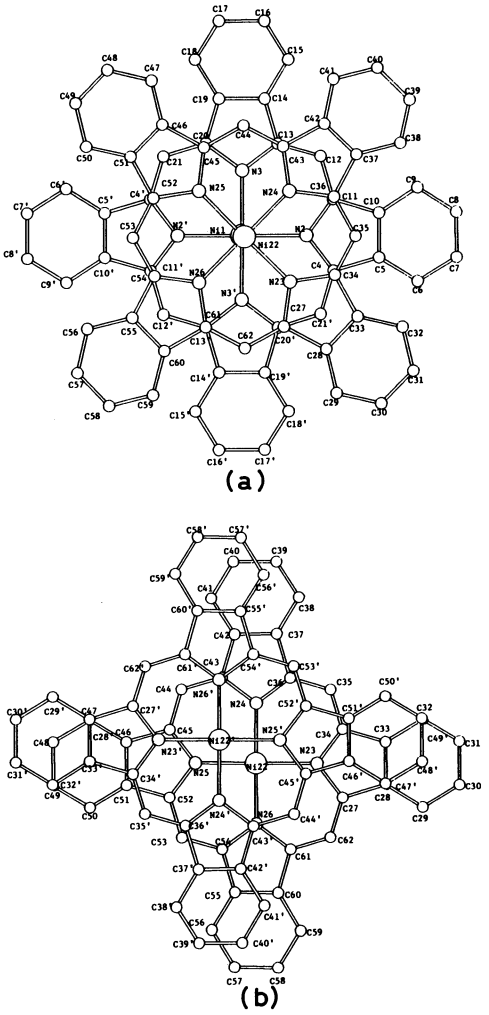

Fig. 2. Overlapping mode of NiTBP's between (a) A and B and (b) B and B′, where A is on the center of symmetry, and B and B′ are interrelated by the center of symmetry.

Table 3. Mean Bond Distances of NiTBP Calculated by Averaging the Chemically Equivalent Bonds

	Molecule A	Molecule B	NiTBPI
Ni-Np	1.976(6)	1.975(6)	1.966(9)
Np-Ca	1.381(11)	1.385(11)	1.391(13)
Ca-Cb	1.455(11)	1.456(12)	1.460(15)
Ca-Cm	1.377(12)	1.367(12)	1.340(15)
Cb-Cb	1.386(11)	1.384(11)	1.391(15)
Cb-Cc	1.405(14)	1.406(14)	1.387(15)
Cc-Cd	1.409(15)	1.395(16)	1.390(16)
Cd-Cd	1.401(15)	1.404(16)	1.391(17)

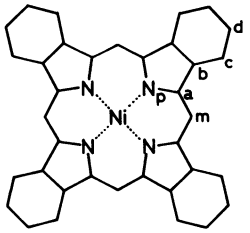

Fig. 2a. This type of overlap is commonly found in the metallo-phthalocyanine iodide (MPcI)[1-3,5] and NiTBP iodide (NiTBPI).[6] The interplanar distance is 3.16 Å, and the Ni-Ni distance is 3.221(2) Å. The molecular overlap between the adjacent trimer is shown in Fig. 2b. The porphyrin skeleton is not twisted but shifted with the interplanar distance of 3.45 Å. This overlapping mode is found in the α-modification of platinum phthalocyanine.[13] The Ni-Ni distance is 3.608(2) Å. The intermolecular atomic distances shorter than 3.4 Å were listed in Table 4. These distances suggest that a charge-transfer interaction exists not only between the molecules A and B but also between B and B'. Figure 3 shows the arrangement of the molecular columns viewed nearly along the c-axis. The NiTBP column is packed pseudo-hexagonally and this packing mode is quite different from those of MPcI and NiTBPI complexes and $(NiPc)_2SbF_6$.[8] The 1-chloronaphthalene molecule is not drawn in Figs. 1 and 3 not to complicate the figure. The solvent molecule is located at the central space, (1/2, 1/2, 1/2) in Fig. 3, the molecular plane making an angle of 57.2° against the NiTBP molecule. The molecular geometry, the an-

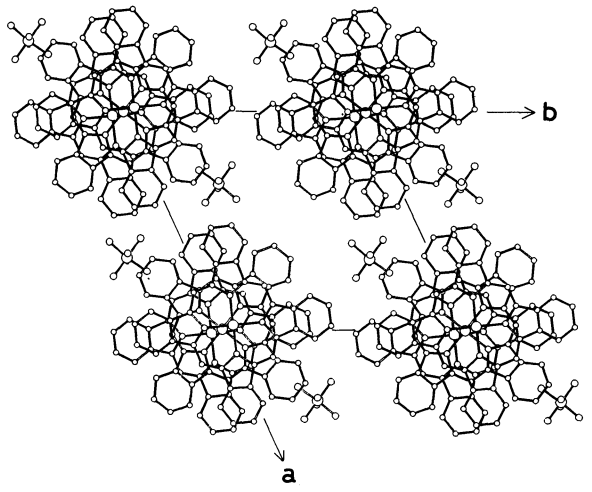

Fig. 3. Projection of the molecules viewed along the c-axis. The solvent molecule which is included in the crystal at around (1/2, 1/2, 1/2) is not drawn in this figure.

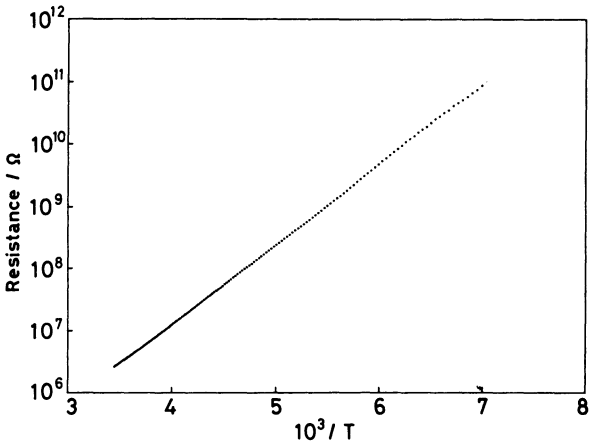

Fig. 4. Temperature dependence of the electrical resistivity.

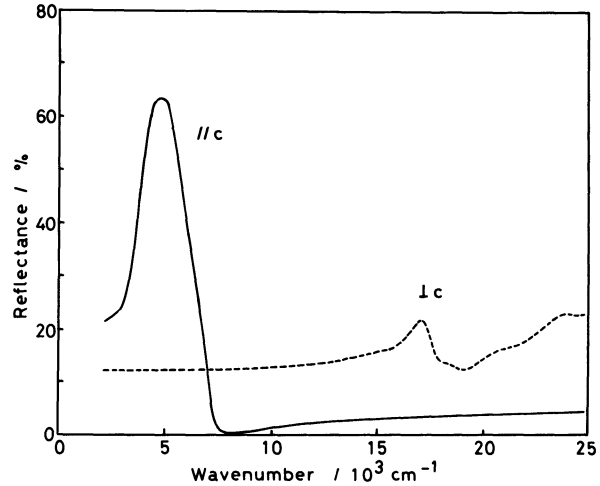

Fig. 5. Polarized reflectance spectrum of $(NiTBP)_3(AsF_6)_2(C_{10}H_7Cl)$.

Table 4. Intermolecular Atomic Distances Shorter than 3.4 Å

		A-B	
Ni(1)-Ni(22)	3.221(2)	C(4)-C(34)	3.214(10)
C(4')-C(52)	3.215(10)	C(10)-C(35)	3.383(9)
C(11)-C(36)	3.213(10)	C(11')-C(54)	3.219(10)
C(12)-C(37)	3.379(12)	C(12)-C(42)	3.352(11)
C(12')-C(55)	3.329(9)	C(12')-C(60)	3.371(10)
C(13)-C(43)	3.209(10)	C(13')-C(61)	3.208(10)
C(14)-C(44)	3.364(9)	C(14')-C(62)	3.399(11)
C(15')-C(59)	3.368(11)	C(19)-C(44)	3.379(11)
C(19')-C(62)	3.362(10)	C(20)-C(45)	3.198(9)
C(20')-C(27)	3.205(10)	C(21)-C(46)	3.310(11)
C(21)-C(51)	3.328(9)	C(21')-C(28)	3.356(10)
C(21')-C(33)	3.388(12)		
		B-B'	
N(23)-C(45')	3.380(8)	N(26)-C(43')	3.341(9)
C(34)-C(51')	3.399(11)	C(36)-C(53')	3.340(11)

isotropic temperature factors, and F_o-F_c data are deposited as Document No. 8791 at the Office of the Editor of Bull. Chem. Soc. Jpn.

The electrical resistivity along the c-axis was 400—1000 ohm cm at room temperature. Figure 4 shows a typical example of the temperature dependence, which indicates the semiconductive behavior. The activation energy of the electrical resistivity was obtained to be 0.26—0.28 eV. If we assume that it is equal to twice the activation energy, the band-gap is estimated to be 0.52—0.56 eV. Figure 5 shows the reflectance spectrum polarized parallel and perpendicular to the c-axis. The //c spectrum exhibited a strong dispersion at about 5000 cm^{-1}, the excitation energy of which is much lower than the lowest intramolecular transition (Q-band) which shows up at 17000 cm^{-1} in the $\perp$c spectrum. Furthermore, this dispersion is completely polarized to the stacking direction. Therefore, this electronic transition is assignable to the charge-transfer (CT) transition. The appearance of the CT transition indicates directly the presence of a strong CT interaction along the stacking direction, in addition to the short intermolecular atomic distances shown in Table 3. Figure 6 shows the optical conductivity spectrum calculated through the Kramers-Kronig transformation of the reflectance spectrum. The FWHM of the CT band is about 1000 cm^{-1} at room temperature, which is extraordinary narrow as compared with organic radical salts.[14-16] The sharp line shape of the CT band means that the electron-molecular vibration coupling is very small. In other words, the distortion of the molecular geometry accompanying the charge transfer is very small. The oscillator strength of the CT absorption band was calculated to be 0.75 per one cation by integrating the conductivity spectrum. This value is considerably larger than the corresponding values: 0.34 for $(BPDT\text{-}TTF)_3(PF_6)_2$[17] and 0.35 of Cs_2TCNQ_3.[18]

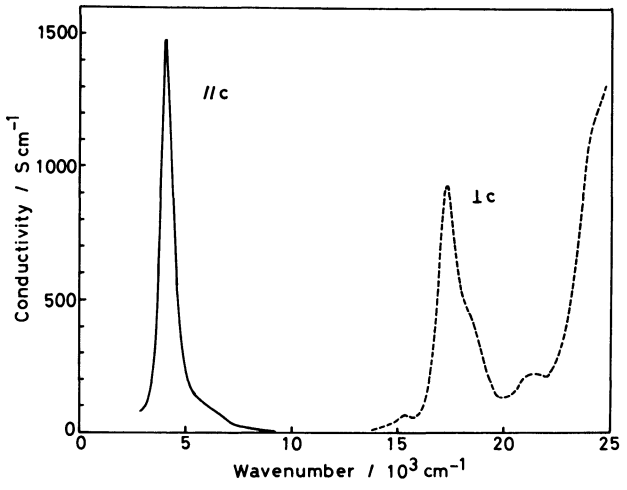

Fig. 6. Optical conductivity spectrum of $(NiTBP)_3(AsF_6)_2(C_{10}H_7Cl)$.

The oscillator strength of the CT band is the measure of the transfer integral. The average transfer integral of $(NiTBP)_3(AsF_6)_2(C_{10}H_7Cl)$ was roughly estimated to be larger than 0.3 eV.[17] A weak ESR signal with a Lorentzian line shape was observed. The g-values were $g//=2.0035$ and $g\perp=2.0014$, and the line widths were $\Gamma//=4.2$ G and $\Gamma\perp=8.0$ G (1G=10^{-4} T), where the static magnetic field was applied parallel and perpendicular to the c-axis. Angle dependence of g-value around the c-axis was very small, and neither g-value nor line width were dependent on temperature. The temperature dependence of the intensity of this signal was Curie-like. The concentration of the unpaired electrons estimated from the temperature dependence of the ESR intensity was 1/1000 molecule^{-1}. Therefore, the large majority of spins on NiTBP forms pairs making non-magnetic ground state, and the origin of the ESR signal is probably attributed to the unpaired electrons trapped at the lattice defects. The g-value of NiTBPI were reported to be $g//=2.060$ and $g\perp=2.018$, and the half width, $\Gamma//=110$ G and $\Gamma\perp=75$ G.[6] In the case of NiTBPI, the unpaired electrons are located both at the Ni atom and at the TBP ligand. The small g-value and the narrow half width of ESR signal in $(NiTBP)_3(AsF_6)_2$-$(C_{10}H_7Cl)$ indicate that the unpaired electrons are located at the TBP ligand. Since the orbital energy of the d_{z^2} is expected to be pressed up by the Ni-Ni interaction, the oxidation part depends probably on the Ni-Ni distance. However, the Ni-Ni distance of this material is almost the same as that (3.217 Å) of NiTBPI.[6] Thus the Madelung energy may also contribute to determine the oxidation part.

The experimental results on the optical spectrum and ESR are quite different from those of organic radical salts like $(BPDT\text{-}TTF)_3(PF_6)_2$[17] and Cs_2-$TCNQ_3$, which are expected to have equivalent electronic structures. For example, Cs_2TCNQ_3 exhibits two CT bands at about 4000 cm^{-1} and 10000 cm^{-1},[18] and presents an ESR signal at room temperature which is attributed to a thermally excited triplet exciton.[19] The appearance of the CT band at higher wavenumber and the small excitation energy of the triplet exciton comes from the large on-site Coulomb energy ($U/4t>1$).[20] However, this material does not exhibit the second CT band despite that the unpaired electrons are making pairs. Therefore, the electronic structure of this material should be understood on the basis of an uncorrelated one-dimensional band model. In this model the CT transition is reinterpreted to be an interband transition and the magnetic activation energy is given by the band gap. This model is in accord with the fact that the band gap estimated from the electrical resistivity agrees quite well with the excitation energy of the optical spectrum. Therefore, we consider that this material have a small on-site Coulomb energy

Table 5. Crystal Growth of Ni(TBP) Complexes by Electrochemical Oxidation

Anion shape	Octahedral	Tetrahedral	Linear
	PF_6 ○	BF_4 ○	Br_3 □
	AsF_6 ○	ClO_4 ○	I_3 □
	SbF_6 □	ReO_4 ○	

○: Single crystal, the typical dimension of which is (0.02—0.09)×(0.02—0.09)×(1—4) mm³. □: Microcrystal, the dimension of which is less than 0.01×0.01×0.5 mm³.

($U/4t<1$), which is related to the large size of the TBP ligand and the large transfer integral.

Other Radical Salts. We prepared several radical salts by using other counter anions. The results on the preparative experiment are shown in Table 5. We examined the structural, electrical, and magnetic properties of the large size of single crystals (X=PF_6, BF_4, ClO_4, and ReO_4) shown in Table 5. The X-ray oscillation photographs showed that the periodic unit along the needle axis were about 9.6 Å. All of these salts are semiconductors with the specific resistivities of 10^3—10^4 ohm cm, and exhibited no ESR signal. These properties quite resembles $(NiTBP)_3(AsF_6)_2$-$(C_{10}H_7Cl)$ which we characterized in this paper. Therefore, we consider that the NiTBP radical salts with octahedral and tetrahedral counter anions shown in Table 5 belong to the same family with $(NiTBP)_3$-$(AsF_6)_2(C_{10}H_7Cl)$.

We deeply thank Prof. Hiroki Haraguchi, Department of Chemistry, the University of Tokyo, and Mr. Yoshimasa Kasahara, Japan Jarrel Ash, Co., for the elemental analysis of Ni and As by means of ICP atomic emission spectroscopy. We are grateful to Prof. Takeshi Miyamoto, Department of Chemistry, the University of Tokyo, for kindly providing us 2-acetylbenzoic acid which is the starting material to synthesize NiTBP.

References

1) C. J. Schramm, R. P. Scaringe, D. R. Stojakovic, B. M. Hoffman, J. A. Ibers, and T. J. Marks, *J. Am. Chem. Soc.*, **102**, 6702 (1980).

2) T. E. Phillips, R. P. Scaringe, B. M. Hoffman, and J. A. Ibers, *J. Am. Chem. Soc.*, **102**, 3435 (1980).

3) J. Martinsen, L. J. Pace, T. E. Phillips, B. M. Hoffman, and J. A. Ibers, *J. Am. Chem. Soc.*, **104**, 83 (1982).

4) J. Martinsen, S. M. Palmer, J. Tanaka, R. C. Greene, and B. M. Hoffman, *Phys. Rev. B*, **30**, 6269 (1984).

5) S. M. Palmer, J. L. Stanton, N. K. Jaggi, B. M. Hoffman, J. A. Ibers, and L. H. Schwartz, *Inorg. Chem.*, **24**, 2040 (1985).

6) J. Martinsen, J. L. Stanton, R. L. Greene, J. Tanaka, B. M. Hoffman, and J. A. Ibers, *J. Am. Chem. Soc.*, **107**, 6915 (1985).

7) T. Inabe, S. Nakamura, W. B. Liang, T. J. Marks, R. L. Burton, C. R. Kannewurf, and K. Imaeda, *J. Am. Chem. Soc.*, **107**, 7224 (1985).

8) K. Yakushi, M. Sakuda, H. Kuroda, A. Kawamoto, and J. Tanaka, *Chem. Lett.*, **1986**, 1161.

9) K. Yakushi, M. Sakuda, I. Hamada, H. Kuroda, A. Kawamoto, J. Tanaka, T. Sugano, and M. Kinoshita, *Synthetic Metals*, **19**, 769 (1987).

10) T. Sakurai and K. Kobayashi, *Rep. Inst. Phys. Chem. Res.*, **55**, 69 (1979).

11) Y. Iyechika, K. Yakushi, and H. Kuroda, *Bull. Chem. Soc. Jpn.*, **53**, 603 (1980).

12) H. Tajima, K. Yakushi, H. Kuroda, G. Saito, and H. Inokuchi, *Solid State Commun.*, **49**, 769 (1984).

13) J. M. Robertson and I. Woodward, *J. Phys. Chem.*, **1940**, 36.

14) K. Yakushi, S. Miyajima, T. Kusaka, and H. Kuroda, *Chem. Phys. Lett.*, **114**, 168 (1985).

15) C. S. Jacobsen, D. B. Tanner, and K. Bechgaard, *Phys. Rev. B*, **28**, 7019 (1983).

16) K. Yakushi, S. Aratani, K. Kikuchi, H. Tajima, and H. Kuroda, *Bull. Chem. Soc. Jpn.*, **59**, 363 (1986).

17) K. Yakushi, H. Tajima, T. Ida, M. Tamura, H. Hayashi, H. Kuroda, A. Kobayashi, H. Kobayashi, and R. Kato, *Synthetic Metals*, in press.

18) K. Yakushi and H. Hayashi, unpublished data.

19) D. B. Chesnut and P. Arthur, Jr., *J. Chem. Phys.*, **36**, 2969 (1962).

20) Z. G. Soos and D. J. Klein, "Molecular Association, Vol. 1," ed by R. Foster, Academic Press, London (1975), p. 1.